Exploring Hamstring Injury Risk using an Inertial Measurement Unit-based Method to obtain Muscle Tendon Unit Lengths and Elongation Velocities in Female Field Hockey Players.

Klaver, J. H.
Master Thesis, TU Delft, Master Mechanical Engineering, Track Haptic Interfaces
Supervisors: Prof. Dr. F. Van der Helm, PhD. A. Seth, MSc. E. Wilmes

Abstract— **Hamstring injuries in field hockey are very common. Accurate estimates of muscle tendon unit lengths (MTU) and elongation velocities could give insight into the risk of injury during field hockey specific movements. For accurate measurements the hockey field would be best suited. Inertial measurement technology allows for such measurements; however, a method of applying this technology to hockey must first be developed and applied to athletes. The goal of this study is to develop this method and indicate what field hockey-related activities might be accompanied with a higher risk for hamstring injuries. Three elite female field hockey athletes participated in this study, performing ten field hockey-specific exercises. The results obtained with inertial measurement technology were compared to the results obtained with the commonly used optoelectric motion capture system. This method showed very good (0.850 - 0.950) to excellent (0.960 - 1.000) coefficients of multiple correlation values. Furthermore, absolute peak values for MTU lengths and elongation velocities were obtained. The results showed that the MTU length and elongation velocity were higher during running while dragging the ball on the hockey stick than during running without ball. The MTU length was also higher during various types of hits than during running. Additionally, the MTU length and elongation velocity were higher on the left leg compared to the right leg. Excessive stretch and high elongation velocities could indicate a greater chance of muscle injuries. This study shows that MTU lengths and elongation velocities can be obtained with inertial measurements and could in part, explain the relatively high hamstring injury rate among female field hockey athletes.**

I. Introduction

A. *Hamstring injuries in field hockey*

In 2013 a study conducted for multiple field hockey tournaments found an average of 29.1 injuries per 1000 hours of sports competitions for female athletes (Theilen et al., 2016). The most frequently injured muscle group within field hockey are the hamstring muscles (Delfino Barboza et al., 2018; Rees et al., 2020). Hamstring strain and hip and groin muscle strains or tears account for 30% of acute muscle injuries, and hamstring tightness was the cause of 11% of all overuse injuries (Delfino Barboza et al., 2018). The semitendinosus, semimembranosus and biceps femoris compose the hamstring muscle group. These muscles originate from the ischial tuberosity and cross both the femoracetabular and tibiofemoral joints (Rodgers et al., 2021). Accurate estimations of muscle mechanics are highly relevant because muscle injuries are believed to occur most frequently during eccentric contraction when the muscles elongate as tension is produced (Liu et al., 2012). Excessive strain in the muscles results in microscopic damage in the muscle fibres (Clark et al., 2008). When this happens frequently, these micro-injuries can result in a more noticeable injury such as a hamstring tear.

Estimates regarding the length and elongation velocities of the hamstring muscles can be derived from the kinematics and injury patterns investigated in many studies. Warman et al. (2019) found that field hockey players spend approximately 80% of a field hockey match in 10 to 60 degrees trunk flexion. Within that range, the torso is flexed at an angle of 30 to 40 degrees for approximately a quarter of the hockey match (Warman et al., 2019). Trunk flexion was defined as the angle between the vertical upright trunk and the flexed trunk. Continuous flexion of the pelvis is expected to lead to increased hamstring muscle tendon unit (MTU) lengths. Furthermore, the field hockey movements are performed asymmetrically with the hockey stick held on the right side of the body. During various types of hits, athletes step out with their right leg forward and left leg trailing. The rules dictate that athletes can only use one side of the hockey stick. For backhand hits, athletes step out with the left leg forward and the right leg trailing. A retrospective analysis study concluded that hamstring injuries were twice as common in the left leg versus the right leg (Wood et al., 2018). Furthermore, a deep forward lunge is incorporated in multiple types of hits (Macleod et al., 2007). The hamstring muscle in the trailing leg elongates during a forward lunge. Therefore, the hamstring muscles are expected to elongate over a larger range of motion during field hockey hits.

Muscle mechanics such as MTU length and elongation velocity could give more insight into the risks of hamstring injuries during field hockey. Using musculoskeletal modelling software, such muscle mechanics can be derived from human movement kinematics. The kinematics can be obtained using movement measurement technology.

B. *Human Motion Analysis*

Human movement research using motion capture technology is commonly performed in a motion capture lab using stereophotogrammetry. One of the existing methods of this technique requires reflective markers on the body segments of the human participant and an optoelectric infrared motion analysis system. Position data is captured and combined with a biomechanical model and used for inverse kinematic calculations to obtain joint and body kinematics. This commonly used measurement method is restricted to laboratory settings. Furthermore, complicated operational procedures and a clear line of sight between the participant and measurement systems are required. Due to these disadvantages the method is not considered favourable for simulating real life complex and interactive movements such as during a field hockey match. However, such movements are considered important when analyzing risk of muscle injury due to the extensive biomechanical loads on the muscles.

Inertial measurement unit (IMU)-based motion analysis is another technology for capturing human movement that can be used outside the laboratory setting. This measurement technology uses IMUs to capture orientation data of the participant's body segments. An IMU is a sensor comprising accelerometers measuring linear acceleration, gyroscopes capturing angular velocity, and magnetometers measuring the magnetic field in three respective orthogonal axes. The information of these sensors is used to determine the angular orientation of the IMU in contrast to stereophotogrammetry which measures position data. The IMUs are attached to corresponding body segments to obtain orientation data of the human movement. The motion of the participants is retrieved by combining the angular orientation information of all the segments' sensors. Because all the measurements take place inside the IMU, which is half the size of a small matchbox, this technology is not bound to a laboratory setting and does not require a clear line of sight. They can measure in versatile settings and during long-distance and long-duration exercises. Therefore they are very useful for capturing human movements during explosive and complex sports movements outside the lab. However, the accuracy and precision of IMU-based motion analysis depends on the type of movement, and the magnitude of the acceleration of the body segments (Cuesta et al., 2010). Also, the proportions and skin impedance of the muscles could contribute to a soft tissue artefact, especially during high-intensity movements (Kamstra., 2022). Movement kinematics are successfully estimated and validated with optoelectric-based measurement technology using IMUs for explosive and complex football-related activities and ice hockey shooting tasks (Wilmes et al., 2020; DenRoche, 2020). However, no studies have assessed the validity of IMU measurements in field hockey-related exercises. Moreover, no research to date has attempted to estimate important muscle properties such as MTU lengths and muscle elongation velocities using IMU technology that contain relevant information to assess muscle injury risk.

This study aims to develop a method to indicate what field hockey-related activities might be accompanied with a higher risk for hamstring injuries using IMUs. Therefore, the primary goal of this study is to compare MTU lengths and elongation velocities of the hamstring muscles obtained with IMU measurements with the results obtained with the commonly used optoelectric measurement technology. The secondary goal of this study is to differentiate between high-risk and low-risk movements for hamstring injuries during field hockey specific movements using the dynamic muscle mechanics obtained with IMU motion tracking technology.

It is hypothesized that similar conclusions can be drawn from the results using IMU-based technology and optoelectric motion capture technology. However, I expect larger differences between the resulting MTU lengths and muscle elongation velocities retrieved from IMU data compared to marker-based data for faster or explosive exercises as seen in previous kinematic oriented studies (Wilmes et al., 2020), because the muscle mechanics will be derived from human kinematics. Secondly, it is hypothesized that the magnitude of MTU length and elongation velocities will be larger for the hamstring muscles in the left leg regarding ball handling movements than the hamstring muscles in the right leg. The difference is expected due to the asymmetrical nature of handling the hockey stick towards the right side of the body. Furthermore, an increase in hamstring length is expected during ball handling exercises versus running due to the frequent flexion of the trunk and the frequently performed deep lunge position during hits.

II. Methods

Three female participants (age $mean = 21.7$ y, $SD = 1.7$, weight $mean = 64.94$ kg, $SD = 2.09$ kg , height $mean = 1.69$ m, $SD = 0.01$ m) participated in this study. All participants were elite field hockey athletes competing at a national level. The participants were injury free for at least six months before participating in this study. All participants were informed about the measurement procedures before and on the day of their measurements. Informed consent in accordance with the Declaration of Helsinki and approved by the ethics committee of the VU Amsterdam was signed by all participants. The study was conducted at the medical centre of the Royal Dutch Football Association (KNVB) in the Netherlands. Two measurement sessions were held for each participant, resulting in six measurement sessions in total.

A. Measurement setup

Twenty-six reflective markers were placed on anatomical landmarks and indicative positions on the participant's body (Wu et al., 2002; Booth et al., 2019). The locations are indicated in Figure 1 and abbreviations are listed in Table I. Double-sided adhesive tape was used to attach the markers to the participant. Two strings of small sports tape (1 cm wide) were used as extra security measures to ensure the markers did not fall off. The reflective markers were captured at 250 Hz with eight infrared cameras of the Vicon Optoelectric System (version 2.7.3, Vicon V5 cameras, Vicon Motion Systems Ltd., Oxford, UK). Two cameras were placed at hip height in front of the participant while the other six cameras were hanging from the ceiling distributed across the lab. An

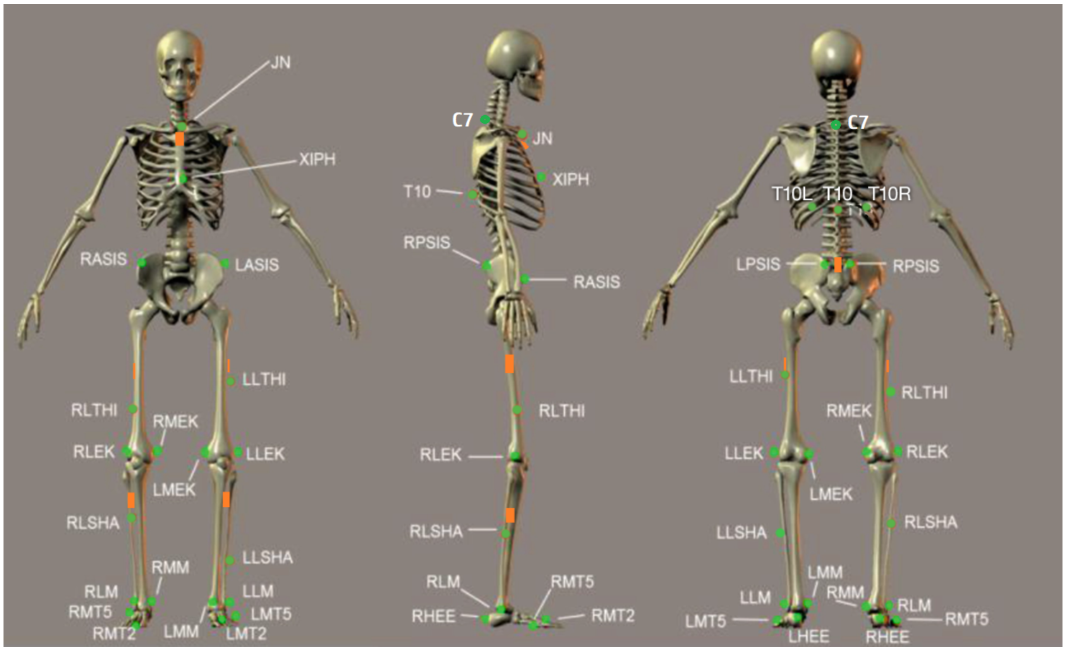

Fig. 1: Anatomical bony landmarks and IMU locations. Edited version, original From Motek Medical, BV Amsterdam, the Netherlands. The bony landmarks and their abbreviations are listed in Table I. The orange squares indicate the positions of the IMUs. These are located on the torso, pelvis, left and right thigh, left and right shank and left and right foot.

TABLE I: Names of the markers place on bony landmark and indicative positions and their abbreviations as used in this paper

Left side markers		**Right side markers**		**Centered markers**	
left metatarsal two	LMT2	right metatarsal two	RMT2	jugular notch	JN
left metatarsal five	LMT5	right metatarsal five	RMT5	xiphoid process	XIPH
left heel	LHEE	right heel	RHEE	cervical spinal segment 7	C7
left lateral malleoli	LLM	right lateral malleoli	RLM	thoracic spinal segment 10	T10
left medial malleoli	LMM	right medial malleoli	RMM		
left lateral femoral epicondyle knee	LLEK	right lateral femoral epicondyle knee	RLEK		
left medial femoral epicondyle knee	LMEK	right medial femoral epicondyle knee	RMEK		
left posterior superior iliac spine	LPSIS	right posterior superior iliac spine	RPSIS		
left anterior superior iliac spine	LASIS	right anterior superior iliac spine	RASIS		
left lateral shank	LLSHA	right lateral shank	RLSHA		
left lateral thigh	LLTHI	right lateral thigh	RLTHI		
left of thoracic spinal segment 10	LT10	right of thoracicspinal segment 10	RT10		

artificial turf mat, commonly used for football practice, lay on the floor.

Eight IMUs (MPU-9150, Invensense, SanJose, CA, USA) were used to measure the orientation angles of the left and right feet, shanks and thighs, and the pelvis and torso. The IMUs were placed on the participant, as shown in Figure 1 and gathered data at 500 Hz. Double-sided adhesive tape was used to attach the sensors to the participant. A single string of sports tape (2.7 cm wide) was pasted over the sensor as an extra measure to make sure the sensors did not fall off during the measurement.

B. Measurement Protocol

A sensor calibration was performed to compensate for misalignment and offsets due to magnetic, or orientation differences in the IMUs (Wilmes et al., 2020; Bastiaansen., 2020). The reflective markers were carefully placed on the participant's body, where after the IMUs were turned on and placed in a box that prevented the sensors from moving. The IMUs were time-synchronized to each other by giving a hard tap on a rigid surface with the box. This action gives a spike in the sensor data, which is recognized during processing (de Ruiter et al., 2019). After synchronizing the IMUs, they are placed on the participant as shown in Figure 1.

The sensors can be placed on the participant in any orientation. A series of movements calibrates the sensors to align the coordinate frame of each sensor with its corresponding body segment frame (Wilmes et al., 2020). First, a static calibration in the neutral pose was done for ten seconds; the longitudinal axis of the body segments is assumed to be equal to the gravitational axis in this position. Next, the participant performed a left thigh-rise, right thigh-rise, and a bow in the sagittal plane ten seconds apart to define the frontal axis. The participant performed the neutral pose in between the movements.

After the calibration of the sensors, a static calibration and range of motion calibration were performed using Vicon Nexus 2. After full calibration, the participant performed ten different field hockey-related movements. First, four basic movements were performed. Namely, the squat, left legged forward lunge, right legged forward lunge and sidestep. Then two running exercises were performed: running with a hockey stick but without a ball at 50 % intensity and running with a hockey stick dragging a hockey ball at 50 % intensity. Lastly, four types of hits are performed: the sweep hit, hit, push, and backhand. A movement was repeated at least four times before continuing to the next movement. More than four trials were performed if the participant made an execution error or the measurement window did not entail the whole movement. Before and after each singular movement (trial), the participant stood in the neutral position for three seconds. After the participant went through all exercises in the first series, a five-minute break was scheduled. The same exercises were repeated in the same order for another four times per exercise after the break. In total, at least eight trials per exercise were performed by each participant. Cones were available to indicate the starting location of the participants.

C. Data Processing

After data collection, the raw marker position data were first processed using Vicon Nexus 2. Possible gaps were filled using the Woltring gap-fill algorithm if gaps were smaller than five frames (0.02 seconds) from Vicon Nexus. Otherwise, the rigid body gap-fill tool was used for gaps smaller than 75 frames (0.3 seconds). If gaps were over 75 frames, the movements were checked manually, and the gaps were filled using the rigid body fill tool and pattern gap-fill tool. Only trials with good marker visibility were used for further processing. The optoelectric marker data was exported and implemented into OpenSim (version 4.2, Stanford University) (Seth et al., 2018; Delp et al., 2007). OpenSim is an open-source software program used for biomechanical modelling of experimental motion data and a valuable tool to gather information about muscles.

First, the generic OpenSim model Rajagopal 2015 was scaled according to the participant's anthropometry (Rajagopal et al., 2016). Anatomical landmarks RTHI, LTHI, RLSHA and LLSHA were not used for scaling. The other markers were paired to estimate the distances between experimental markers relative to the distances between corresponding virtual markers. The marker pairs used are shown in Table II. Then inverse kinematic (IK) calculations were performed in OpenSim. For the optoelectric motion capture data, generalized joint coordinate values for each time step of a movement were calculated using a weighted least squares problem minimizing marker errors using the Inverse Kinematics Tool. The weight of the LASIS, RASIS, LPSIS and RPSIS markers were set at four, the weight of markers RTHI, LTHI, RLSHA and LLSHA were set at 0.25. All other markers had a weight of one.

For IMU data processing, IMU-based data was exported to Matlab (version 2018a, The MathWorks, Inc., Natick, MA, USA). The IMU-based data was cut in subsets the length of the corresponding optoelectric based trial data. Throughout the movement, the knee and hip angles were cross-correlated to synchronize the trials from IMU and marker-based measurements. After processing and calibration in Matlab, the previously scaled model (scaled based on marker data) was calibrated for processing IMU-based data. First, the scaled model was put in the default position using the static trial from the optoelectric measurements. Secondly, the calibration was done using the IMU Placer Tool in OpenSim; the pelvis IMU was used as base unit in the minus z-direction, and a static trial of the IMU-based data was implemented (Al Borno et al., 2022). The IMU-based data was processed using OpenSim's corresponding IMU Inverse Kinematics Tool, minimizing orientation errors (Al Borno et al., 2022). The resulting kinematics from IK were analyzed using the Analyze Tool and filtered with 6 Hz in OpenSim to obtain the lengths of the muscle-tendon units of the hamstring muscles; semitendinosus, semimembranosus and biceps femoris long head. The numerical derivative of the MTU length over time was obtained via finite differencing to estimate the elongation velocities of each muscle.

D. Data Analysis

After data processing, the root mean square differences (RMSD) and coefficient of multiple correlations (CMC) values (Ferrari et al., 2010) were calculated for each trial to find the differences between the results of the IMU-based measurement system and the optoelectric measurement system. By calculating the CMC values for each exercise, the similarity of the trials can be assessed, taking differences in offset into account between the measurement methods (Wilmes et al., 2020). The interpretation of the CMC values was as follows: weak (<0.650); moderate (0.650-750); good(0.750 - 0.850); very good (0.850-0.950); excellent(0.95 - 1.00) (Ferrari et al., 2010). Out of the at least eight performed trials, the trials with very deviating results were examined if the RMSDs were above 1.99 cm and/or the CMC values were weak. These trials showed either misalignment of the optoelectric and IMU-based data or a non-recorded trial and were discarded. The misalignment was caused by an incorrect cross-correlation of kinematic angles during data processing and not due to dissimilarity of the data. The four last performed trials of the remaining trials were selected for each movement and were used for data analysis to compare optoelectric and IMU-based data for each session. The last trials of each movement were selected for the purpose of consistency over all participants and to control for the possibility of a learning effect throughout the measurement session. First, the arithmetic mean and standard deviations of the RMSDs over these four trials were calculated. The arithmetic mean and standard deviations over the resulting values were used for between-subject analysis and are presented in this paper. The average over the CMC values of the four trials was also calculated. Fishers Z was calculated first to prevent underestimation the means of the CMC values (Silver et al., 1987). The arithmetic mean of the resulting Z-values was then transformed back to the correlation coefficient (Silver et al., 1987). The average of the resulting values was used for between-subject analysis and presented in this paper.

TABLE II: Typical marker pairs for scaling the generic model to the participant's body proportions. The body segments are scaled in the X, Y and Z direction or uniform. The patella and talus are not scaled and have a scale factor of 1.0

Measurement	Marker Pairs			
torso x	JN - C7	XIPH - T10		
torso y	C7 - T10	C7 - LPSIS	C7 - RPSIS	XIPH - JN
torso z	T10 - LT10	T10 - RT10		
pelvis x	LPSIS - LASIS	RPSIS - RASIS		
pelvis y	LPSIS - RASIS	RPSIS - LASIS		
pelvis z	RASIS - LASIS	RPSIS - LPSIS		
thigh left x	LASIS - LPSIS			
thigh left y	LMEK - LLEK			
thigh left z	LMEK - LLEK			
thigh right x	RASIS - RPSIS			
thigh right y	RMEK - RLEK			
thigh right z	RMEK - RLEK			
tibia left xz	LLM - LMM	LMEK - LLEK		
tibia left y	LLEK - LLM			
tibia right xz	RLM - RMM	RLEK - RMEK		
tibia right y	RLEK - RLM			
calcaneus left uniform	LHEE - LLM	LHEE - LMT2	LHEE - LMT5	
calcaneus right uniform	RHEE - RLM	RHEE - RMT2	RHEE - RMT5	

The maximal and minimal values for the MTU lengths of the hamstring muscles were calculated for the same four trials that were used for comparing IMU and optoelectric-based data to analyze the exercises' effect on the lengthening of the muscle. The peak contraction velocity and the peak elongation velocity were also calculated for each of those four trials. The arithmetic means and standard deviations for the MTU lengths and muscle elongation velocity over the four trials of each exercise are first determined for each participant individually. The arithmetic means and standard deviations for the MTU length and velocity per exercise over all participants are determined next, using the formerly calculated mean values of each individual participant. The arithmetic means and standard deviations over all participants will be used for between-subject analysis and presented in this paper.

III. Results

A. Optoelectric versus IMU-based measurements

Out of six measurement sessions, five were used to compare optoelectric-based data to IMU-based data. A sensor malfunctioned during one session out of the remaining five sessions. Therefore, only two trials were used for data processing for this particular session. These trials will account for half of the weight compared to the other measurement sessions when calculating the mean of the RMSDs and CMC values.

Mean RMSDs (cm), and CMC values of the MTU lengths of each hamstring muscle on the left and right leg are shown in Table III and V, respectively. Furthermore, the mean RMSDs (cm/s) and CMC values for the elongation velocities of each hamstring muscle on the left and right leg are shown in Table IV and VI. The RMSDs for MTU length are all below one centimeter for both legs with one exception for the right semitendinosus muscle while running without the ball (Table III, V). The RMSDs for the MTU length do appear more or less consistent for all exercises. However, for the left leg ($mean = 0.59$ cm, $SD = 0.13$ cm) RMSDs are slightly lower compared to the right leg ($mean = 0.71$ cm, $SD = 0.14$ cm) with the most notable difference during running without the ball ($mean = 0.75$ cm, $SD = 0.08$ cm, $mean = 1.00$ cm, $SD = 0.09$ cm, left and right leg respectively). The RMSD of the MTU length of the relative basic and slow movements like the squat, lunge and side step appear to have a lower RMSD ($mean = 0.56$ cm, $SD = 0.11$ cm) then the complex and faster movements such as running and the various types of hits ($mean = 0.71$ cm, $SD = 0.14$ cm). The between-subjects standard deviations of the RMSDs for the MTU length range from 0.05 cm to 0.30 cm.

The CMC values for the MTU lengths show high correlation values across all exercises ($mean = 0.963$ $SD = 0.029$) with low between-subjects standard deviations. There is no observable difference in CMC values between the left and right leg or movement types. The RMSDs for the muscle elongation velocities range from 1.21 cm/s to 15.60 cm/s. There appears to be a significant relation between the RMSD values of a movement type and the execution velocity of the movement. Slower executed trials such as squat, lunge and side step ($mean = 1.69$ cm/s $SD = 0.33$ cm/s) have a lower RMSD while faster trials such as various types of hits ($mean = 6.10$ cm/s, $SD = 1.53$ cm/s) have an increased RMSD. The running trials which are performed with the highest execution velocity show RMSD values over ten times higher compared to the basic movements ($mean = 10.60$ cm/s, $SD = 2.34$ cm/s). The RMSD values for the left leg ($mean = 4.89$ cm/s, $SD = 3.26$ cm/s) are slightly lower compared to the right leg ($mean = 5.58$ cm/s, $SD = 3.93$ cm/s). The between-subjects standard deviations range from 0.15 cm/s to 4.96 cm/s and increases for faster and more complex movement types but remains more or less proportional to the mean RMSD. The CMC values for the muscle elongation velocities show high correlation between optoelectric-based measurement data and IMU-based measurement data ($mean = 0.962$, $SD = 0.020$). There is no observable difference between the left and right leg or between the type of movement. The between-subjects standard deviations for the CMC values are also low across all exercises and muscles.

TABLE III: Mean of the root mean square differences (RMSD) and coefficients of multiple correlation (CMC) between the muscle tendon unit (MTU) lengths obtained by processing optoelectronic and inertial measurement unit (IMU)-based movement data from the left leg. The mean and between participant standard deviation are shown obtained from all participants.

	semitendinosus left		**semimembranosus left**		**Biceps femoris left**	
Exercise	RMSD (cm)	CMC	RMSD (cm)	CMC	RMSD (cm)	CMC
squat	0.61 ± 0.05	0.934 ± 0.018	0.47 ± 0.04	0.933 ± 0.014	0.54 ± 0.08	0.976 ± 0.005
lunge right	0.38 ± 0.16	0.997 ± 0.005	0.32 ± 0.13	0.996 ± 0.004	0.41 ± 0.10	0.989 ± 0.008
lunge left	0.55 ± 0.23	0.964 ± 0.065	0.44 ± 0.16	0.966 ± 0.052	0.53 ± 0.22	0.973 ± 0.035
side step	0.73 ± 0.12	0.921 ± 0.049	0.57 ± 0.10	0.918 ± 0.052	0.62 ± 0.11	0.970 ± 0.012
run without ball	0.87 ± 0.20	0.987 ± 0.005	0.68 ± 0.18	0.989 ± 0.005	0.70 ± 0.14	0.988 ± 0.007
run with ball	0.69 ± 0.17	0.993 ± 0.004	0.55 ± 0.15	0.994 ± 0.004	0.57 ± 0.15	0.994 ± 0.004
sweep hit	0.86 ± 0.22	0.982 ± 0.010	0.69 ± 0.19	0.982 ± 0.009	0.70 ± 0.16	0.985 ± 0.007
hit	0.71 ± 0.26	0.985 ± 0.017	0.57 ± 0.21	0.985 ± 0.015	0.60 ± 0.19	0.984 ± 0.015
push	0.78 ± 0.29	0.987 ± 0.013	0.61 ± 0.23	0.988 ± 0.013	0.63 ± 0.20	0.987 ± 0.011
backhand	0.56 ± 0.13	0.976 ± 0.022	0.44 ± 0.10	0.979 ± 0.017	0.50 ± 0.13	0.977 ± 0.023

TABLE IV: Mean of the root mean square differences (RMSD) and coefficients of multiple correlation (CMC) between the contraction velocities obtained by processing optoelectronic and inertial measurement unit (IMU)-based movement data from the left leg. The mean and between participant standard deviation are shown obtained from all participants.

	semitendinosus left		**semimembranosus left**		**Biceps femoris left**	
Exercise	RMSD (cm/s)	CMC	RMSD (cm/s)	CMC	RMSD (cm/s)	CMC
squat	1.60 ± 0.20	0.952 ± 0.004	1.24 ± 0.16	0.954 ± 0.005	1.44 ± 0.22	0.977 ± 0.006
lunge right	1.58 ± 1.27	0.991 ± 0.018	1.28 ± 1.05	0.992 ± 0.018	1.41 ± 1.01	0.982 ± 0.035
lunge left	1.90 ± 0.25	0.990 ± 0.003	1.48 ± 0.21	0.991 ± 0.003	1.69 ± 0.10	0.979 ± 0.004
side step	2.31 ± 0.89	0.933 ± 0.057	1.84 ± 0.75	0.933 ± 0.065	1.90 ± 0.52	0.954 ± 0.028
run without ball	12.77 ± 3.62	0.978 ± 0.008	10.13 ± 3.43	0.981 ± 0.010	9.62 ± 2.27	0.980 ± 0.007
run with ball	9.47 ± 2.57	0.990 ± 0.005	7.43 ± 2.25	0.991 ± 0.006	6.82 ± 1.61	0.992 ± 0.004
sweep hit	7.95 ± 4.62	0.966 ± 0.061	6.45 ± 3.77	0.967 ± 0.060	5.72 ± 3.03	0.969 ± 0.048
hit	7.27 ± 4.14	0.975 ± 0.067	5.85 ± 3.26	0.974 ± 0.064	5.34 ± 2.71	0.973 ± 0.058
push	8.70 ± 4.96	0.980 ± 0.035	7.08 ± 3.97	0.981 ± 0.034	6.39 ± 3.06	0.980 ± 0.029
backhand	3.84 ± 1.19	0.980 ± 0.027	3.12 ± 1.03	0.982 ± 0.025	3.09 ± 0.79	0.975 ± 0.029

TABLE V: Mean of the root mean square differences (RMSD) and coefficients of multiple correlation (CMC) between the muscle tendon unit (MTU) lengths obtained by processing optoelectronic and inertial-based movement data from the right leg. The mean and between participant standard deviation are shown obtained from all participants.

	semitendinosus right		**semimembranosus right**		**Biceps femoris right**	
Exercise	RMSD (cm)	CMC	RMSD (cm)	CMC	RMSD (cm)	CMC
squat	0.65 ± 0.10	0.903 ± 0.059	0.53 ± 0.06	0.896 ± 0.055	0.57 ± 0.09	0.969 ± 0.011
lunge right	0.61 ± 0.18	0.946 ± 0.038	0.48 ± 0.14	0.953 ± 0.030	0.57 ± 0.17	0.963 ± 0.027
lunge left	0.75 ± 0.24	0.983 ± 0.011	0.59 ± 0.18	0.986 ± 0.008	0.66 ± 0.20	0.967 ± 0.014
side step	0.74 ± 0.16	0.922 ± 0.069	0.63 ± 0.12	0.907 ± 0.077	0.61 ± 0.11	0.970 ± 0.016
run without ball	1.13 ± 0.30	0.976 ± 0.010	0.92 ± 0.29	0.979 ± 0.010	0.95 ± 0.14	0.972 ± 0.013
run with ball	0.85 ± 0.23	0.988 ± 0.007	0.68 ± 0.20	0.990 ± 0.006	0.68 ± 0.20	0.989 ± 0.007
sweep hit	0.90 ± 0.19	0.943 ± 0.030	0.71 ± 0.15	0.952 ± 0.023	0.72 ± 0.17	0.957 ± 0.024
hit	0.82 ± 0.17	0.964 ± 0.013	0.64 ± 0.13	0.972 ± 0.011	0.68 ± 0.09	0.966 ± 0.007
push	0.83 ± 0.27	0.979 ± 0.012	0.65 ± 0.22	0.983 ± 0.011	0.67 ± 0.18	0.979 ± 0.009
backhand	0.75 ± 0.23	0.984 ± 0.008	0.60 ± 0.17	0.985 ± 0.006	0.67 ± 0.19	0.986 ± 0.007

TABLE VI: Mean of the root mean square differences (RMSD) and coefficients of multiple correlation (CMC) between the contraction velocities obtained by processing optoelectronic and inertial-based movement data from the right leg. The mean and between participant standard deviation are shown obtained from all participants.

	semitendinosus right		**semimembranosus right**		**Biceps femoris right**	
Exercise	RMSD (cm/s)	CMC	RMSD (cm/s)	CMC	RMSD (cm/s)	CMC
squat	1.48 ± 0.23	0.947 ± 0.017	1.21 ± 0.19	0.948 ± 0.017	1.32 ± 0.15	0.975 ± 0.003
lunge right	2.51 ± 1.38	0.982 ± 0.030	1.96 ± 1.15	0.985 ± 0.027	1.99 ± 0.75	0.968 ± 0.027
lunge left	1.97 ± 0.42	0.981 ± 0.007	1.54 ± 0.32	0.984 ± 0.007	1.65 ± 0.35	0.968 ± 0.014
side step	2.01 ± 0.58	0.953 ± 0.027	1.62 ± 0.51	0.956 ± 0.029	1.62 ± 0.39	0.965 ± 0.018
run without ball	15.60 ± 3.26	0.966 ± 0.018	12.37 ± 3.21	0.970 ± 0.015	11.87 ± 1.32	0.966 ± 0.026
run with ball	12.02 ± 3.28	0.982 ± 0.013	9.64 ± 2.62	0.983 ± 0.011	9.42 ± 2.22	0.981 ± 0.014
sweep hit	7.69 ± 3.14	0.940 ± 0.057	6.15 ± 2.61	0.947 ± 0.055	5.71 ± 2.02	0.936 ± 0.043
hit	7.66 ± 3.15	0.953 ± 0.062	6.04 ± 2.74	0.960 ± 0.061	5.91 ± 2.08	0.947 ± 0.047
push	8.70 ± 3.68	0.969 ± 0.021	7.00 ± 3.20	0.972 ± 0.022	6.61 ± 2.39	0.966 ± 0.013
backhand	5.42 ± 1.01	0.973 ± 0.007	4.31 ± 0.95	0.975 ± 0.010	4.37 ± 0.77	0.970 ± 0.009

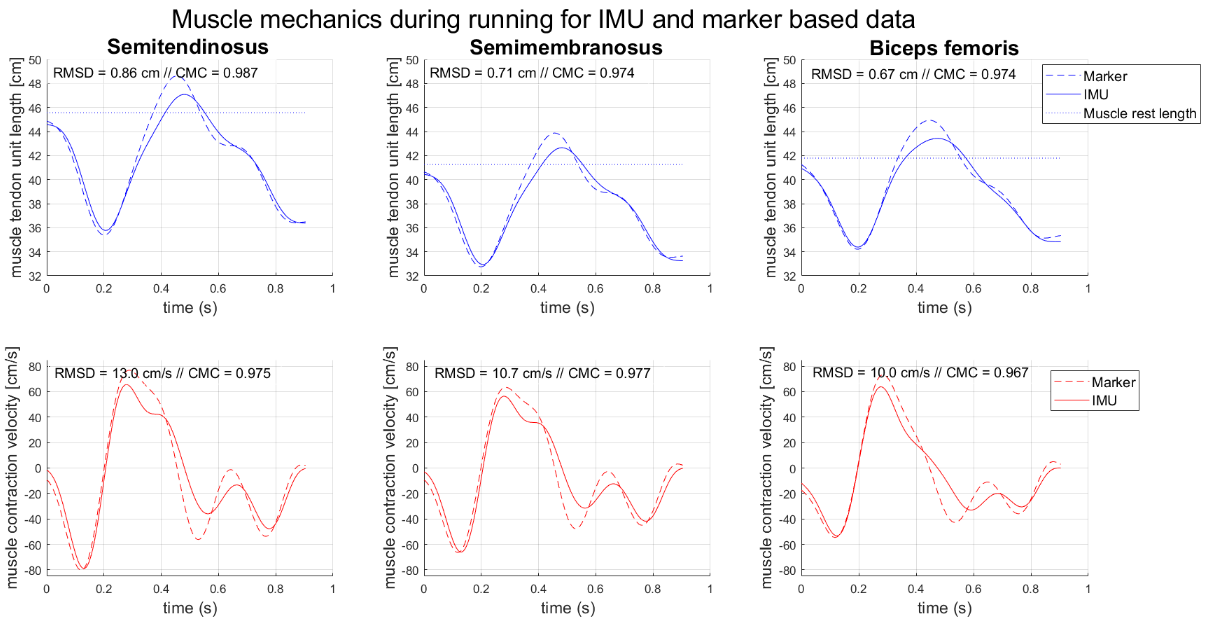

Fig. 2: Typical results for muscle tendon unit lengths and muscle elongation velocity during running without a ball performed by one participant. The results obtained with marker data are shown with the dashed line, the results obtained with inertial measurement unit (IMU) data are shown with the continuous line, and in the top three graphs, the muscle tendon unit's rest length is shown with the dotted line. The coefficient of multiple correlations (CMC) and root mean square difference (RMSD) is indicated in the respective graph.

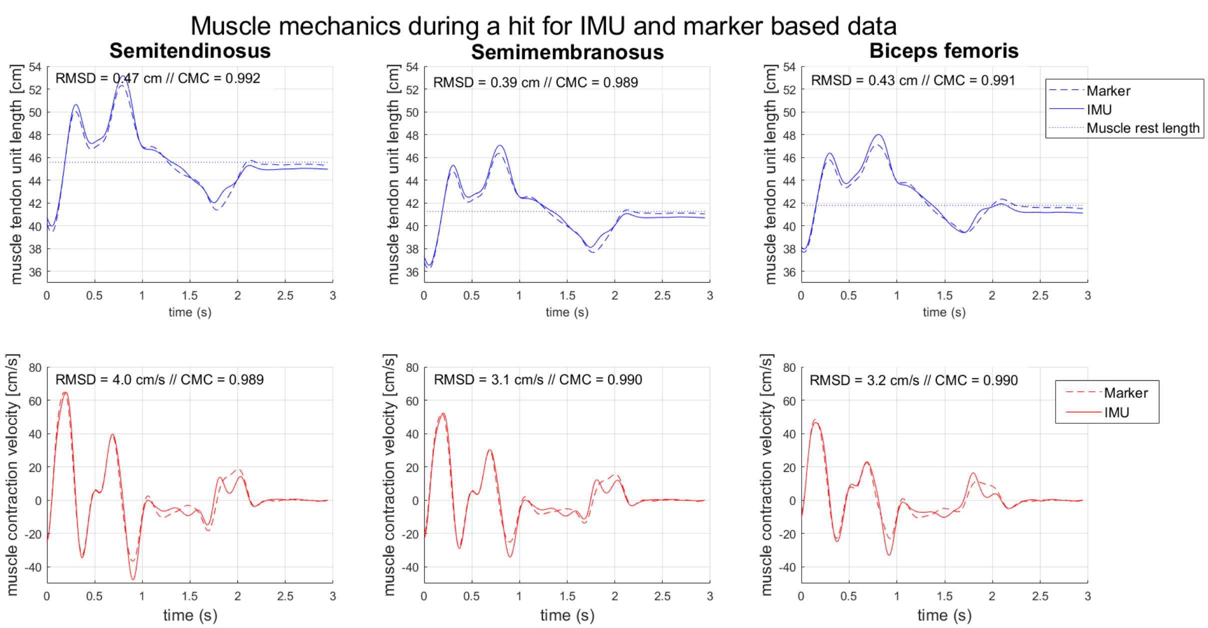

Fig. 3: Typical results for muscle tendon unit lengths and muscle elongation velocity during a hit performed by one participant. The results obtained with marker data are shown with the dashed line, the results obtained with inertial measurement unit (IMU) data are shown with the continuous line, and in the top three graphs, the muscle tendon unit's rest length is shown with the dotted line. The coefficient of multiple correlations (CMC) and root mean square difference (RMSD) is indicated in the respective graph.

TABLE VII: Mean peak values the muscle tendon unit length of the hamstring muscles of the left leg during several movement types

	Semitendinosus left		Semimembranosus left		Biceps femoris left	
rest length (cm)	44.4 ± 0.7		40.2 ± 0.7		40.4 ± 0.7	
Exercise	Max length (cm)	Min length (cm)	Max length (cm)	Min length (cm)	Max length (cm)	Min length (cm)
run without ball	48.0 ± 0.7	36.4 ± 1.3	43.3 ± 0.6	33.6 ± 1.2	44.2 ± 0.6	34.8 ± 1.2
run with ball	49.5 ± 1.1	37.1 ± 0.9	44.5 ± 1.0	34.1 ± 0.8	45.5 ± 0.9	35.5 ± 0.8
push	51.5 ± 0.9	39.0 ± 1.3	45.9 ± 0.8	35.8 ± 1.1	46.9 ± 0.7	37.1 ± 1.2
hit	51.0 ± 1.2	39.4 ± 0.3	45.3 ± 1.0	36.1 ± 0.3	46.2 ± 1.0	37.4 ± 0.4
sweep hit	51.9 ± 1.0	39.7 ± 1.3	46.0 ± 0.8	36.4 ± 1.1	47.2 ± 0.8	37.6 ± 1.1

TABLE VIII: Mean peak values of the muscle tendon unit length of the hamstring muscles of the right leg during several movement types

	Semitendinosus right		Semimembranosus right		Biceps femoris right	
rest length (cm)	44.5 ± 0.006		40.2 ± 0.006		40.5 ± 0.006	
Exercise	Max length (cm)	Min length (cm)	Max length (cm)	Min length (cm)	Max length (cm)	Min length (cm)
run without ball	46.8 ± 0.7	36.7 ± 1.9	42.3 ± 0.5	33.5 ± 1.6	43.1 ± 0.6	35.1 ± 1.7
run with ball	49.4 ± 0.9	38.0 ± 1.6	44.3 ± 0.7	34.6 ± 1.3	45.2 ± 0.8	36.2 ± 1.4
push	50.6 ± 0.7	40.5 ± 0.6	45.3 ± 0.6	36.6 ± 0.6	46.3 ± 0.8	38.2 ± 0.6
hit	49.6 ± 0.6	41.0 ± 0.7	44.5 ± 0.6	37.0 ± 0.8	45.3 ± 0.7	38.3 ± 0.8
sweep hit	50.2 ± 0.8	42.3 ± 0.2	45.0 ± 0.7	38.1 ± 0.2	46.1 ± 0.8	39.4 ± 0.2

TABLE IX: Mean peak values of elongation velocities of the hamstring muscles of the left leg during several movement types

	Semitendinosus left		Semimembranosus left		Biceps femoris left	
Exercise	Max velocity (cm/s)	Min velocity (cm/s)	Max velocity (cm/s)	Min velocity (cm/s)	Max velocity (cm/s)	Min velocity (cm/s)
run without ball	66.9 ± 10.8	-65.4 ± 15.1	55.6 ± 9.5	-53.9 ± 12.7	61.8 ± 11.6	-44.0 ± 10.6
run with ball	75.2 ± 7.5	-56.7 ± 7.4	62.1 ± 5.5	-47.6 ± 7.1	63.9 ± 5.2	-40.2 ± 3.1
push	71.8 ± 13.8	-44.8 ± 4.8	58.3 ± 11.5	-37.5 ± 4.4	55.3 ± 11.1	-33.0 ± 2.4
hit	63.4 ± 10.2	-39.0 ± 4.2	50.5 ± 8.5	-31.1 ± 3.7	48.7 ± 7.4	-28.2 ± 2.3
sweep hit	57.7 ± 8.7	-34.5 ± 6.1	46.3 ± 7.1	-28.9 ± 5.6	44.1 ± 6.2	-25.1 ± 2.9

TABLE X: Mean peak values of elongation velocities of the hamstring muscles of the right leg during several movement types

	Semitendinosus right		Semimembranosus right		Biceps femoris right	
Exercise	Max velocity (cm/s)	Min velocity (cm/s)	Max velocity (cm/s)	Min velocity (cm/s)	Max velocity (cm/s)	Min velocity (cm/s)
run without ball	57.5 ± 9.2	-62.0 ± 16.6	48.7 ± 8.3	-52.5 ± 13.7	50.5 ± 14.5	-40.2 ± 12.3
run with ball	72.7 ± 6.7	-57.8 ± 7.7	60.5 ± 5.3	-48.7 ± 6.5	60.2 ± 11.8	-42.1 ± 4.9
push	52.1 ± 5.2	-37.6 ± 3.3	44.4 ± 4.0	-32.2 ± 2.5	34.6 ± 5.9	-29.1 ± 4.5
hit	44.0 ± 5.2	-36.1 ± 6.5	37.8 ± 4.2	-31.8 ± 6.6	29.1 ± 5.0	-28.4 ± 7.2
sweep hit	41.8 ± 5.8	-28.3 ± 2.3	35.8 ± 4.8	-24.2 ± 1.8	27.5 ± 4.6	-21.1 ± 2.5

B. Muscle tendon unit lengths and muscle elongation velocities

Examples of the MTU length and elongation velocities for running without the ball and for the hit performed by one of the participants are shown in Figure 2 and 3, respectively. The results for running, running with the ball, push, hit and sweep hit are presented in this paper.

In Table XI and XII the mean peak values and the rest lengths of the left and right hamstring muscles are shown, respectively. The peak values for elongation velocities are shown in Table XIV and XIII. The positive peak values show the muscle velocity while the muscle is elongating, the negative peak values show the muscle velocity while the muscle is contracting. For clarity, I chose only to show the results based on IMU measurements for five selected exercises. The results from optoelectric-based measurements and the remaining exercises are shown in the appendix. In Figure 4 the maximal and minimal values of the semitendinosus muscle are shown, visualising the operating range of the left and right side for five exercises. Similar graphs for the semimembranosus and biceps femoris muscles are shown in the appendix.

First of all, it is notable that the maximal MTU lengths are higher and the minimal MTU lengths are lower for running without the ball compared to running with the ball (Table XI,XII). This results in a slightly increased operating range as visualised for the semitendinosus muscle in Figure 4. When comparing the running exercises to the various types of hits, it is observed that the maximal and minimal values are higher (Table XI,XII). The higher maximal and lower minimal values for the left leg (Table XI) compared to the right leg (Table XII) result in a larger range of motion for the muscles in the left leg (visualised for the semitendinosus muscle in Figure 4).

In Table XIV and XIII a higher maximal elongation velocity is observed for running with the ball compared to running without. For all muscles except the right biceps femoris a higher minimal elongation velocity is observed as well (Table XIV, XIII). The minimal elongation velocity values for the various types of hits are higher compared to the running

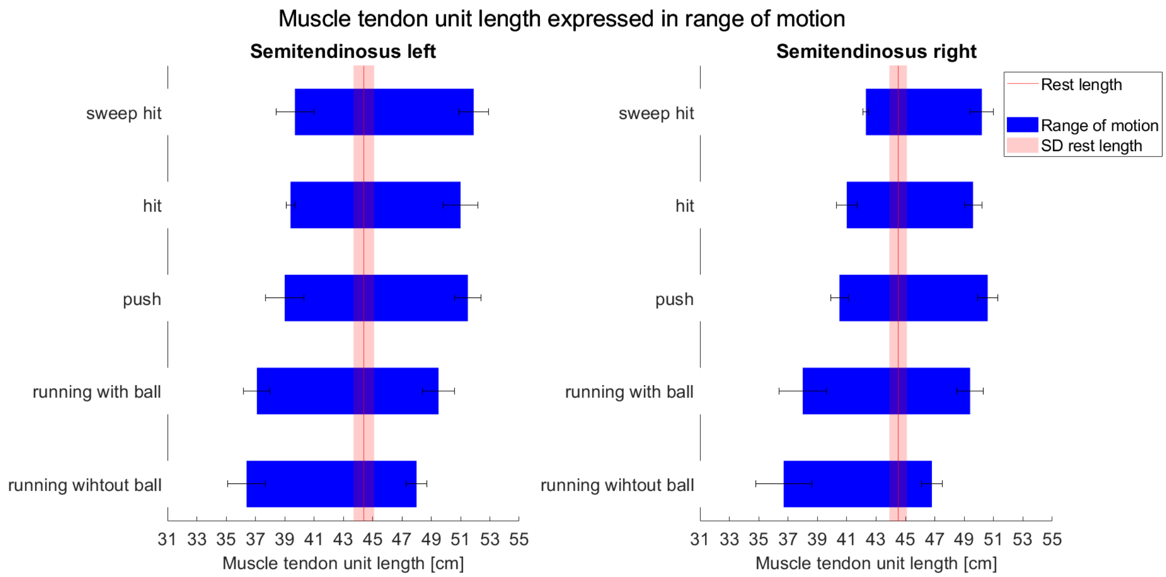

Fig. 4: Operating range of the left and right semitendinosus muscle tendon unit. The blue bars indicate the muscle's range of motion as mean over all the participants. The red vertical line indicates the mean rest length of the muscles.

exercises (Table XIV, XIII). The maximal muscle velocities are lower for the types of hits compared to running except for the left semitendinosus muscle and semimembranosus muscle during the hit. The maximal velocity values on the left leg are higher compared to the maximal values on the right leg (Table XIV, XIII), resulting in a larger muscle velocity range on the left side. This is especially evident for the various types of hits (Table XI,XIII).

IV. Discussion

This study aimed to develop a method to indicate what field hockey-related activities might be accompanied with a higher risk for hamstring injuries using IMUs.

A. *Comparison IMU-based measurements*

The primary goal of this study was to compare MTU lengths and muscle elongation velocities obtained with IMU measurements with the results from a similar procedure using an optoelectric infrared motion analysis system. The results of this comparison showed very good to excellent CMC values and small RMSDs between IMU-based and optoelectric-based data. The RMSDs for MTU lengths increased slightly in relation to the complexity and execution velocity of the movements, which is in accordance with the hypothesis.

Findings in other studies investigating human movement kinematics can support the RMSDs and CMC values found in the present paper (Wilmes et al., 2020; DenRoche, 2020). Wilmes et al. (2020) investigated the validity of IMU measurements against optoelectric measurements for human movement kinematics in football. He proposed two explanations for an increase in RMSD. Firstly, linear accelerations can influence the sensor's orientation estimation because of assumptions made in sensor fusion algorithms. The measured acceleration direction is assumed to be the direction of the gravitational acceleration (Madgwick et al., 2011). Secondly, the soft tissue between the sensors on the skin and the subject's bones deforms while performing a movement and could lead to a soft tissue artefact. Wilmes' paper did not find an increase in RMSDs with increasing movement intensity, but this could be explained because the lowest intensity exercise he measured was performed at an already high intensity of 50 %. Another study by DenRoche (2020) assessed IMU measurement validation against optoelectric measurement technology in ice hockey shooting tasks and found that the RMSD of the gravitational axis was significantly larger compared to other Cartesian axis (DenRoche, 2020). The increased RMSDs in this paper could be present due to the influence of linear acceleration on the estimated IMU orientation or the soft tissue artefact because the resulting muscle mechanics were determined using the kinematics of the field hockey-related movements.

Both these studies calculated the CMC values for their respective sports-related kinematics. The results of Wilmes showed good validity and very good to excellent correlations. The study of DenRoche showed moderate to very good correlations depending on the axis. This study, however, used a different biomechanical model for the each measurement method. The differences in these models were assumed to be the reason for the large relative errors. In the present study, I used the same biomechanical model to accurately compare the two measurement methods. The model was scaled based on marker data and used for both marker-based inverse kinematics and IMU-based inverse kinematics. After the kinematics were calculated, the data was processed for both measurement techniques in the same manner. Because of the differences in the biomechanical models in DenRoche's study and the equality of the models in the present study, the CMC values obtained in the present study were logically higher compared to the study of DenRoche.

However, the statistical power of both Wilmes' and DenRoche's studies were presumably higher due to the larger amount of participants. The results and conclusions of the present study can be used as an indication and inspiration for further research but should not be interpreted as validation of the used method. Because the scaling method used in this study was unpractical for measurements outside the laboratory setting, the generic model can also be scaled and posed visually in OpenSim using photographs. In future research the model scaling and calibration should be independent of marker-based measurements. With this addition, IMU-based research methods could be further developed and used for estimating MTU lengths and muscle elongation velocities during sports activities outside the lab setting.

B. *Injury risk*

The secondary goal of this study was to differentiate between high-risk and low-risk movements for hamstring injuries during field hockey specific movements using the dynamic muscle properties obtained with IMU motion tracking technology. To get an indication of the risk, the maximal and minimal MTU lengths and elongation velocities were obtained during field hockey specific movements.

The results showed that the hamstring muscles have larger maximal MTU lengths when running with the ball compared to running without. Meanwhile, the velocity range remained the same throughout the respective movements while the positive and negative peak values increased. Furthermore, the various types of hits were compared to the running exercises. The results showed that the hamstring muscles were stretched more during the various types of hits as opposed to running. However, the velocity range was smaller with lower maximal velocity peak values. This means that the muscles elongate at a lower velocity before the maximal MTU length was reached for the various types of hits compared to running. Excessive stretch and high elongation velocities have been found to be risk factors for muscle injuries (Liu et al., 2012). A biomechanical study researched muscle strain in rabbits and found that eccentric contraction was the primary cause of muscle strain injury (Garrett et al., 1987). Another study investigated the effect of elongation speed on muscle strain injury in rabbits. They found that when the injury occurred, an increase in muscle contraction force was accompanied by an increase in elongation speed (Best et al., 1995). The severity of muscle strain injury was also positively correlated to elongation speed in eccentric contraction (Brooks et al., 2001).

Large MTU lengths and high muscle elongation velocities were both associated with increased risk of injury on their own. However, the risk increases even more when both occur simultaneously (Liu et al., 2012). Therefore, the risk of injury during running with the ball or the various types of hits appeared to be higher compared to running exercises. This is also supported by the high incidence of hamstring injuries during running and sprinting (Yeung et al., 2009). An increase in MTU lengths and elongation velocities is presumed to add stress and load on the muscles and fatigue the hamstrings even further, making injury more likely.

The range of motion and the maximal elongation velocities were larger for the left leg during field hockey specific exercises. This means that the muscles elongate at a higher velocity range in the left leg before reaching higher maximal MTU lengths. This outcome is in line with my hypothesis, in which I expected higher MTU lengths and elongation velocities on the left leg, based on the asymmetric handling of the hockey stick. Additionally, it explains how it is possible that hip and hamstring injuries happen twice as often on the left leg compared to the right leg (Wood et al., 2018). This paper shows that hamstring MTU lengths and elongation velocities can be obtained using IMU technology. The higher MTU lengths and elongation velocities during the field hockey specific movements may explain the relatively high hamstring injury incidence in field hockey players (Theilen et al., 2016). Similar conclusions could be drawn from the marker data shown in the appendix.

There were several limitations to this study. The artificial turf in the lab was meant for football instead of field hockey. The artificial grass was higher and more resistant when dragging the ball than a field hockey field. The underground could have influenced the participants' performance when a hockey ball was involved in the exercise. The movements were possibly performed less naturally due to the ball's higher drag force. Also, as previously mentioned, the measurements were done inside a lab. On-field measurements should be conducted to measure human movement that better resembles field hockey competitions and training.

Future research should consider including electromyography (EMG) measurements to determine when the muscles are activated during elongation. EMG measures the action potential of the muscle during contraction, indicating the moment of eccentric contraction during muscle elongation. A shorter duration of the muscle activation increases the severity of the muscle injury (Liu et al., 2012; Lovering et al., 2005). EMG measurements could therefore give more insight into the severity and moment of injury during eccentric contraction (Lovering et al., 2005). Muscle force output can also be calculated in OpenSim using the Computed Muscle Control Tool and ground reaction force data. This addition could give further insightful information relevant to hamstring injury risk.

V. Conclusion

This study introduced a method to assess hamstring MTU lengths and elongation velocities during field hockey specific movements using inertial measurement units. High MTU lengths and elongation velocities may indicate an increased risk for muscle injury. It was evident that the highest MTU lengths and elongation velocities were present during running with the ball and the various types of hits. The following conclusions can be drawn from this paper:

- The high MTU lengths and elongation velocities during running with the ball and the various hit types could in part explain the relatively high hamstring injury rate among female field hockey athletes.
- The introduced method showed good similarity to the commonly used stereophotogrammetry and thus could open possibilities for more in-depth IMU-based injury risk assessment on the field.

Acknowledgements

The author would like to thankfully acknowledge the Dutch Royal Football Association (KNVB) for facilitating the research programme by giving access to their research facilities.

References

Al Borno, M., O'Day, J., Ibarra, V., Dunne, J., Seth, A., Habib, A., ... & Delp, S. (2022). OpenSense: An open-source toolbox for Inertial-Measurement-Unit-based measurement of lower extremity kinematics over long durations. *Journal of neuroengineering and rehabilitation, 19*(1), 1-11.

Bastiaansen, B. J., Wilmes, E., Brink, M. S., de Ruiter, C. J., Savelsbergh, G. J., Steijlen, A., ... & Lemmink, K. A. (2020). An inertial measurement unit based method to estimate hip and knee joint kinematics in team sport athletes on the field. *JoVE (Journal of Visualized Experiments)*, (159), e60857.

Best, T. M., McElhaney, J. H., Garrett Jr, W. E., & Myers, B. S. (1995). Axial strain measurements in skeletal muscle at various strain rates

Booth, A. T. C., van der Krogt, M. M., Buizer, A. I., Steenbrink, F., & Harlaar, J. (2019). The validity and usability of an eight marker model for avatar-based biofeedback gait training. *Clinical Biomechanics, 70,* 146-152.

Brooks, S. V., & Faulkner, J. A. (2001). Severity of contraction-induced injury is affected by velocity only during stretches of large strain. *Journal of Applied Physiology, 91*(2), 661-666.

Clark, R. A. (2008). Hamstring injuries: risk assessment and injury prevention. *Annals Academy of Medicine Singapore, 37*(4), 341.

Cross, K. M., Gurka, K. K., Conaway, M., & Ingersoll, C. D. (2010). Hamstring strain incidence between genders and sports in NCAA athletics. *Athletic training & sports health care, 2*(3), 124-130.

Cuesta-Vargas, A. I., Galán-Mercant, A., & Williams, J. M. (2010). The use of inertial sensors system for human motion analysis. *Physical Therapy Reviews, 15*(6), 462-473.

Delfino Barboza, S., Nauta, J., van der Pols, M. J., van Mechelen, W., & Verhagen, E. A. L. M. (2018). Injuries in Dutch elite field hockey players: a prospective cohort study. *Scandinavian journal of medicine & science in sports*, 28(6), 1708-1714.

Delp, S. L., Anderson, F. C., Arnold, A. S., Loan, P., Habib, A., John, C. T., ... & Thelen, D. G. (2007). OpenSim: open-source software to create and analyze dynamic simulations of movement. *IEEE transactions on biomedical engineering, 54*(11), 1940-1950.

Denroche, S. K. (2020). Evaluating the use of inertial measurement unit technology during an ice hockey shooting task. McGill University.

Ferrari, A., Cutti, A. G., & Cappello, A. (2010). A new formulation of the coefficient of multiple correlation to assess the similarity of waveforms measured synchronously by different motion analysis protocols. *Gait & posture, 31*(4), 540-542.

Ferrari, A., Cutti, A. G., Garofalo, P., Raggi, M., Heijboer, M., Cappello, A., & Davalli, A. (2010). First in vivo assessment of "Outwalk": a novel protocol for clinical gait analysis based on inertial and magnetic sensors. *Medical & biological engineering & computing, 48*(1), 1-15.

Garrett JR, W. E., Safran, M. R., Seaber, A. V., Glisson, R. R., & Ribbeck, B. M. (1987). Biomechanical comparison of stimulated and nonstimulated skeletal muscle pulled to failure. *The American journal of sports medicine, 15*(5), 448-454.

Kamstra, H., Wilmes, E., van der Helm, F. (2022). Quantification of Error Sources with Inertia Measurement Units in Sports

Liu, H., Garrett, W. E., Moorman, C. T., & Yu, B. (2012). Injury rate, mechanism, and risk factors of hamstring strain injuries in sports: a review of the literature. *Journal of sport and health science, 1*(2), 92-101.

Lovering, R. M., Hakim, M., Moorman III, C. T., & De Deyne, P. G. (2005). The contribution of contractile pre-activation to loss of function after a single lengthening contraction. *Journal of biomechanics, 38*(7), 1501-1507.

MacLeod, H., Bussell, C., & Sunderland, C. (2007). Time-motion analysis of elite women's field hockey, with particular reference to maximum intensity movement patterns. *International Journal of Performance Analysis in Sport, 7*(2), 1-12.

Madgwick, S. O., Harrison, A. J., & Vaidyanathan, R. (2011, June). Estimation of IMU and MARG orientation using a gradient descent algorithm. In *2011 IEEE international conference on rehabilitation robotics* (pp. 1-7). IEEE.

Rajagopal, A., Dembia, C. L., DeMers, M. S., Delp, D. D., Hicks, J. L., & Delp, S. L. (2016). Full-body musculoskeletal model for muscle-driven simulation of human gait. *IEEE transactions on biomedical engineering, 63*(10), 2068-2079.

Rees, H., McCarthy Persson, U., Delahunt, E., Boreham, C., & Blake, C. (2020). Epidemiology of injuries in senior men's field hockey: A two-season prospective observational injury surveillance study. *Journal of sports sciences, 38*(24), 2842-2849.

Rees, H., McCarthy Persson, U., Delahunt, E., Boreham, C., & Blake, C. (2021). The burden of injury in field hockey: A secondary analysis of prospective cohort data. *Scandinavian Journal of Medicine & Science in Sports, 31*(4), 884-893.

Rodgers, C. D., & Raja, A. (2021). Anatomy, bony pelvis and lower limb, hamstring muscle. *StatPearls [Internet].*

de Ruiter, C. J., & van Dieën, J. H. (2019). Stride and step length obtained with inertial measurement units during maximal sprint acceleration. *Sports, 7*(9), 202.

Seth, A., Hicks, J. L., Uchida, T. K., Habib, A., Dembia, C. L., Dunne, J. J., ... & Delp, S. L. (2018). OpenSim:

Simulating musculoskeletal dynamics and neuromuscular control to study human and animal movement. *PLoS computational biology, 14*(7), e1006223.

Silver, N. C., & Dunlap, W. P. (1987). Averaging correlation coefficients: should Fisher's z transformation be used?. *Journal of applied psychology, 72*(1), 146.

Theilen, T. M., Mueller-Eising, W., Bettink, P. W., & Rolle, U. (2016). Injury data of major international field hockey tournaments. *British journal of sports medicine, 50*(11), 657-660.

Warman, G. E., Cole, M. H., Johnston, R. D., Chalkley, D., & Pepping, G. J. (2019). Using microtechnology to quantify torso angle during match-play in field hockey. *The Journal of Strength & Conditioning Research*, 33(10), 2648-2654.

Wilmes, E., de Ruiter, C. J., Bastiaansen, B. J., van Zon, J. F., Vegter, R. J., Brink, M. S., ... & Savelsbergh, G. J. (2020). Inertial sensor-based motion tracking in football with movement intensity quantification. *Sensors, 20*(9), 2527.

Wood, M., Althorpe, T., Hatch, M., Ness, S., McPhee, R., & Minchinson, S. (2018). A multifactorial appraisal of injury data of upper hamstring and hip injuries in elite field hockey players. *Journal of Science and Medicine in Sport, 21*, S80.

Yeung, S. S., Suen, A. M., & Yeung, E. W. (2009). A prospective cohort study of hamstring injuries in competitive sprinters: preseason muscle imbalance as a possible risk factor. *British journal of sports medicine, 43*(8), 589-594.

Wu, G., Siegler, S., Allard, P., Kirtley, C., Leardini, A., Rosenbaum, D., ... & Stokes, I. (2002). ISB recommendation on definitions of joint coordinate system of various joints for the reporting of human joint motion—part I: ankle, hip, and spine. *Journal of biomechanics, 35*(4), 543-548.

VI. Appendix

TABLE XI: Mean peak values the muscle tendon unit length of the hamstring muscles of the left leg during several movement types obtained with optoelectric measurements

	Semitendinosus left		**Semimembranosus left**		**Biceps femoris left**	
rest length (m)	44.4 ± 0.8		40.2 ± 0.8		40.5 ± 0.9	
Exercise	Max length (cm)	Min length (cm)	Max length (cm)	Min length (cm)	Max length (cm)	Min length (cm)
run without ball	48.3 ± 0.7	35.8 ± 1.3	43.5 ± 0.7	33.0 ± 1.1	44.5 ± 0.7	34.5 ± 1.1
run with ball	49.6 ± 0.6	36.9 ± 0.7	44.6 ± 0.6	33.9 ± 0.6	45.6 ± 0.5	35.5 ± 0.6
push	51.3 ± 0.6	38.7 ± 1.0	45.7 ± 0.6	35.5 ± 0.8	46.6 ± 0.5	37.0 ± 0.9
hit	50.8 ± 0.7	39.0 ± 0.4	45.2 ± 0.6	35.8 ± 0.5	45.9 ± 0.6	37.2 ± 0.4
sweep hit	51.8 ± 0.9	39.4 ± 0.8	46.0 ± 0.8	36.1 ± 0.8	46.9 ± 0.8	37.5 ± 0.8

TABLE XII: Mean peak values of the muscle tendon unit length of the hamstring muscles of the right leg during several movement types obtained with optoelectric measurements

	Semitendinosus right		**Semimembranosus right**		**Biceps femoris right**	
rest length (m)	44.5 ± 0.007		40.2 ± 0.008		40.5 ± 0.008	
Exercise	Max length (cm)	Min length (cm)	Max length (cm)	Min length (cm)	Max length (cm)	Min length (cm)
run without ball	47.7 ± 0.8	35.2 ± 1.2	42.9 ± 0.7	32.4 ± 1.2	43.8 ± 1.0	34.0 ± 1.2
run with ball	49.7 ± 0.8	37.1 ± 0.7	44.5 ± 0.8	33.9 ± 0.7	45.8 ± 0.7	35.5 ± 0.7
push	50.7 ± 0.8	39.6 ± 0.5	45.2 ± 0.8	36.0 ± 0.4	46.2 ± 0.9	37.6 ± 0.4
hit	49.6 ± 0.8	40.1 ± 0.6	44.4 ± 0.8	36.3 ± 0.7	45.3 ± 0.8	37.7 ± 0.8
sweep hit	50.3 ± 0.7	41.4 ± 0.6	44.9 ± 0.8	37.4 ± 0.5	46.0 ± 0.9	38.9 ± 0.5

TABLE XIII: Mean peak values of elongation velocities of the hamstring muscles of the left leg during several movement types obtained with optoelectric measurements

	Semitendinosus left		**Semimembranosus left**		**Biceps femoris left**	
Exercise	Max velocity (cm/s)	Min velocity (cm/s)	Max velocity (cm/s)	Min velocity (cm/s)	Max velocity (cm/s)	Min velocity (cm/s)
run without ball	76.2 ± 13.5	-69.5 ± 10.4	62.5 ± 10.7	-56.9 ± 10.7	66.0 ± 15.4	-46.4 ± 8.5
run with ball	81.8 ± 4.0	-58.3 ± 6.3	67.0 ± 3.4	-49.0 ± 3.4	66.0 ± 5.9	-40.2 ± 4.3
push	69.9 ± 11.8	-45.6 ± 5.3	56.7 ± 10.1	-37.7 ± 10.1	50.8 ± 9.7	-31.4 ± 2.5
hit	63.3 ± 7.5	-38.9 ± 2.9	50.7 ± 6.5	-31.0 ± 6.5	47.0 ± 5.9	-27.3 ± 3.1
sweep hit	58.9 ± 6.7	-33.5 ± 2.5	47.2 ± 5.8	-27.8 ± 5.8	43.3 ± 5.0	-23.0 ± 3.6

TABLE XIV: Mean peak values of elongation velocities of the hamstring muscles of the right leg during several movement types obtained with optoelectric measurements

	Semitendinosus right		**Semimembranosus right**		**Biceps femoris right**	
Exercise	Max velocity (cm/s)	Min velocity c(m/s)	Max velocity (cm/s)	Min velocity (cm/s)	Max velocity (cm/s)	Min velocity (cm/s)
run without ball	67.5 ± 14.5	-68.2 ± 10.4	58.7 ± 11.8	-56.5 ± 8.9	60.8 ± 14.1	-45.6 ± 7.9
run with ball	86.5 ± 3.1	-58.8 ± 3.6	71.0 ± 2.5	-48.6 ± 3.1	67.4 ± 5.1	-41.4 ± 1.7
push	60.4 ± 6.8	-42.1 ± 3.3	50.4 ± 5.5	-35.0 ± 3.0	42.1 ± 7.2	-30.0 ± 4.0
hit	53.7 ± 8.7	-42.5 ± 4.9	44.9 ± 7.2	-35.3 ± 4.5	36.7 ± 7.3	-30.9 ± 7.2
sweep hit	50.2 ± 7.2	-34.9 ± 4.1	41.9 ± 6.0	-28.8 ± 3.2	33.9 ± 6.3	-22.5 ± 1.5

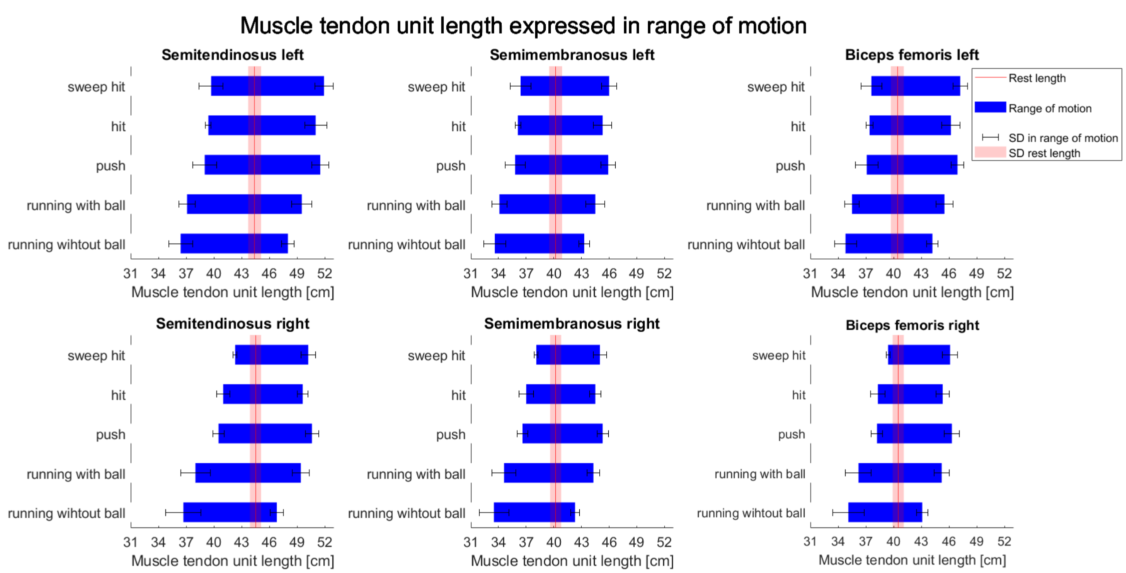

Fig. 5: Operating range of the left and right hamstring muscle tendon units. The blue bars indicate the muscle's range of motion as mean over all the participants. The red vertical line indicates the mean rest length of the muscle over all participants.

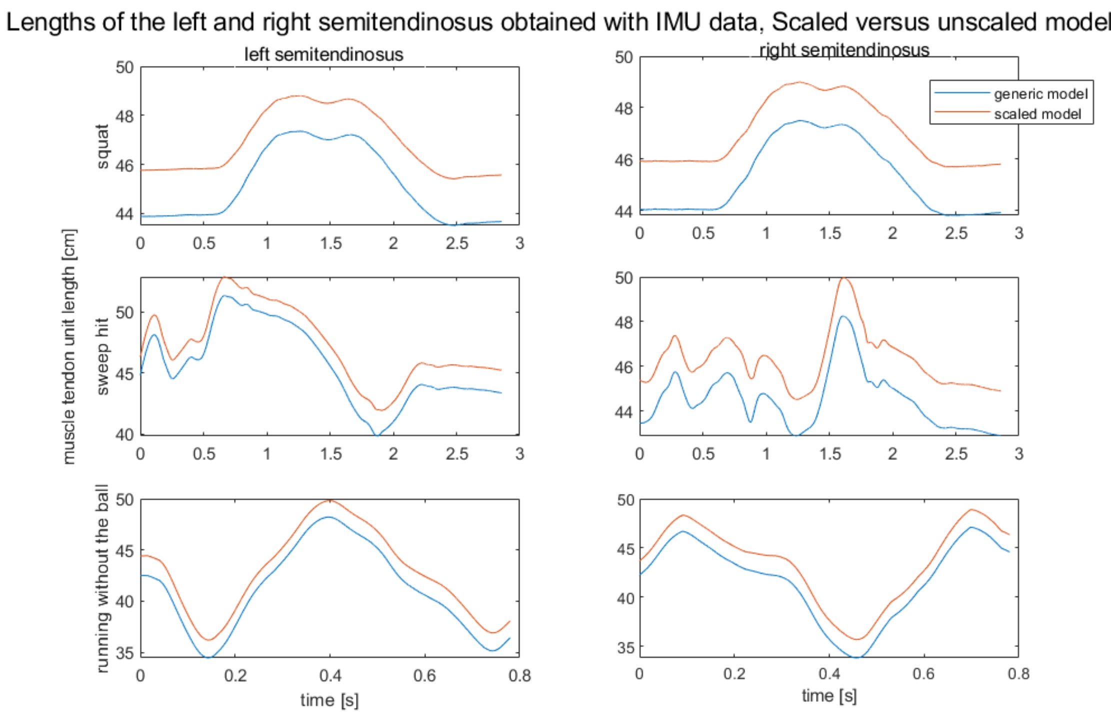

Fig. 6: Individual trials of one of the participants are shown for the squat, sweep hit and running with the ball. The blue graphs show the trials where IMU inverse kinematics is done on a generic model, which is put in default position with visual aid. Photographs in the static position from before the measurements were used. These photos were not taken during the static pose and were not very detailed. The red graphs show the same trials processed using a scaled model (scaled with marker data) put in default position with marker data, after which IMU inverse kinematics is done. The offset between the graphs for the same trial in this figure illustrates the importance of the default position and scaling of the model.